ISSN 0915-633X

NATIONAL INSTITUTE FOR FUSION SCIENCE

Evolution of Magnetic Islands in a Heliac

T. Hayashi, T. Sato, H.J. Gardner and J.D. Meiss

(Received - Aug. 26, 1994)

NIFS-308 Sep. 1994

RESEARCH REPORT
NIFS Series

NAGOYA, JAPAN

EVOLUTION OF MAGNETIC ISLANDS IN A HELIAC

T. HAYASHI and T. SATO

National Institute for Fusion Science,
Furocho, Nagoya 464-01, Japan

H.J. GARDNER

Plasma Research Laboratory and Department of Theoretical Physics,
Research School of Physical Sciences and Engineering,
Australian National University,
Canberra, ACT 0200, Australia

and

J.D. MEISS

Department of Applied Mathematics,
University of Colorado,
Boulder, Colorado 80309

Abstract

Simulations of three-dimensional equilibria in the H-1 Heliac with the HINT code show that the size of a dangerous magnetic island should increase with plasma pressure but that a destruction of the equilibrium at low β is avoided because the rotational transform evolves to exclude the rational surface concerned. At higher pressures there is evidence of near-resonant flux surface deformations which may lead to an equilibrium limit. A reconnected equilibrium at still higher pressures exhibits a double island structure which is similar to homoclinic phase portraits which have been observed after separatrix reconnection in Hamiltonian systems.

keyword: heliac, three dimensional equilibrium, magnetic island, self-healing of magnetic island, finite pressure effect, homoclinic bifurcation, stellarator

I. INTRODUCTION

An important goal of the experimental program of the present, and next generation of stellarators is the investigation of the behaviour of magnetic islands and their effect on plasma confinement. This is particularly the case for the low-shear experiments such as the Heliac where the presence of low-order rational surfaces could lead to the growth of islands which have widths which are an appreciable fraction of the plasma minor radius. In their benign mode, these large magnetic islands might be associated with a localized flattening of the plasma pressure gradient which would reduce the plasma $<\beta>$ (β is the ratio of plasma pressure to magnetic pressure, and the bracket denotes the volume averaged value). In more serious instances, overlapping islands could lead to global stochasticity and a loss of confinement.

The HINT[1] three-dimensional MHD equilibrium code has been previously applied to study the evolution of magnetic islands in heliotron/torsatron[2–4] and Helias[4–6] equilibria. An important physics result for both configurations was that self-healing of magnetic islands could occur at finite pressures. The finite-pressure island chains appeared to have a phase which was independent of their phase in the vacuum magnetic field. In situations where these phases were opposite, the island widths shrunk as the plasma β increased and then grew again, with their natural phase, at higher pressures.

The Heliac configuration has a large spatial excursion about a central conductor and flux surfaces which look generally bean-shaped in their minor cross-section. It is distinguished by its deep magnetic well which, for example, in the 3-period H-1 Heliac[7] can be varied continuously from a 1% magnetic hill to a 6% magnetic well in the vacuum field. The strong coupling between toroidal and helical curvatures means that the magnetic flux surfaces of the toroidal Heliac are more complicated than either heliotron/torsatron or Helias and, as such, the application of HINT to the H-1 configuration described here can be seen as a test of the robustness and reliability of that code. It can also be seen as a test of the robustness of the H-1 surfaces themselves. In particular, we have been motivated to examine the extent to which the critical $<\beta> = 1\%$ stability limits forecast for H-1[8,9] correspond to an equilibrium limit set by the growth of islands. A further motivation was to determine whether self-healing occurred for H-1. This is particularly important, in the light of the earlier HINT results, because field-line-tracing studies for vacuum fields of H-1 have yet to show any variation of the phase of the major magnetic islands across the parameter space of H-1 (in the absence of field errors)[10].

In this paper, calculation results show appearance of a variety of topology in magnetic islands induced in finite β equilibria. In the Appendix, we discuss such variation in the topology can be reproduced by a standard nontwist map.

II. THE MODEL

The HINT code takes as input the components of the vacuum magnetic field along a given boundary and an initial guess for the pressure profile.[5] For the Heliac, the large helical excursion of the plasma combined with a central set of conductors meant that the conventional twisting-rectangular boundary of HINT had to be generalized to a polygonal one with a large helical pitch. We have modified the code accordingly, and the outline of this boundary shape for H-1 can be seen in Fig. 1. The normal components of the magnetic field along the boundary are held fixed during the finite β simulation (i.e. it is considered to be a perfect conductor). The plasma pressure profile is implemented by advancing a pair of relaxation equations along magnetic field lines with the result that the pressure profile flattens automatically inside an island. The initial guess for the pressure profile chosen was $p = p_0(1-\psi)^2$ where ψ is the normalized toroidal flux. (This profile is kept with a good numerical accuracy during the relaxation if magnetic islands do not appear.) This meant that $<\beta> \approx \beta_0/3$ depending on the width of islands, where β_0 denotes the value of β averaged along the magnetic axis. Calculations were carried out for one half-period of the machine, assuming stellarator symmetry.

We examined a particular H-1 configuration which included the island structure corresponding to the (rotational transform) $\iota = 6/5$ resonance in the vacuum field. Two cross-sections of this ($\phi = 0$ and $\frac{\pi}{3}$, ϕ is the toroidal angle), are shown in Fig. 1. The central conductors have a major radius of 1 meter and the aspect ratio of the configuration is about 7. The slightly larger cross-section is on the inboard side of the machine. This model configuration is obtained from the "standard" configuration of H-1[8] by increasing the current in the helical trim coil to 3% of the main central current. Figure 2 shows the rotational transform for this vacuum configuration, indicating that the profile is monotonous in the vacuum field and the magnetic shear is quite small. There is a uniform magnetic well of about 1% across the flux surfaces shown. The rigid feature of the island's phase is the o-point on the outboard centre-line of the right-hand cross section. The major island chains with even and odd numbers of lobes appear to have an o-point with this symmetry under all combinations of currents in the H-1 coils[10].

The HINT code was run with a grid of 73×73 points in each poloidal plane and 41 points in the toroidal direction. Field-line tracing, to produce the puncture plots shown

below, was performed using a 6th order Runge-Kutta method. Typical runs at a fixed plasma β converged in 50 Alfvén times. Convergence studies in the grid to 109×109×59 points were performed with no qualitative change in the results.

III. RESULTS AND DISCUSSION

The results of the HINT simulations are shown in Figs. 3 to 11. When β increases, the value of the rotational transform at the magnetic axis ι_0 increases, while the value of that at around half the minor radius tends to decrease slightly. The value of ι near the plasma boundary does not change significantly. This behavior in the ι profile results in appearance of the minimum of ι (vanishing shear) at around half the minor radius. The value of the minimum ι shows quite subtle behavior as a function of β; as is shown in the following, depending on the value of the minimum ι with respect to 6/5, the most dangerous (low order) rational surface relevant, a variety of topology appears for magnetic islands induced in finite β equilibria.

Figure 3, at $\beta_0 = 1.5\%$, shows that the size of the $\iota = 6/5$ island should increase with plasma pressure to about 1/5 of the plasma radius. The corresponding ι profile is shown in Fig. 4, indicating that the shear is vanishingly small around $\iota = 6/5$. The pressure contours are shown in Fig. 5. The good agreement between the pressure and flux surfaces in Figs. 3 and 5 is a verification of the validity of the HINT simulation.

If the pressure is increased to $\beta_0 = 2.0\%$, in Fig. 6, the plasma appears to experience a form of self-healing, however the corresponding ι profile, in Fig. 7, shows that this is because the 6/5 surface has been excluded from the configuration. It is possible that this exclusion might be due to some self-consistent plasma dynamics and, as such, could be considered as a (new) form of self-healing. As the pressure is increased further, in Figs. 8 and 9, the HINT results show that the minimum value of ι remains just above 6/5, however the flux surfaces show marked signs of *near-resonant* deformation. At the $\beta_0 = 3.8\%$ of Fig. 8 the deformation is extreme and the plasma is probably at its equilibrium limit.

The tendency of the H-1 vacuum island chain to grow as the pressure increases should be contrasted with the TJ-II Heliac.[11] The particular TJ-II configuration included a large 4/3 island which appeared to be opposite in phase to the H-1 islands considered here, indicating a possible occurence of the self-healing in finite β equilibria. A comparison of this aspect of the island dynamics of the H-1 and TJ-II Heliacs could become an important part of the experimental program of the two devices.

Figures 10 and 11 show the flux surfaces and ι profile when the equilibrium pressure is increased to $\beta_0 = 4.4\%$. The flux surfaces have reconnected to form a double island structure which is analogous to the homoclinic phase portraits observed for Hamiltonian dynamical systems after separatrix reconnection[12], but appears to be new in the context of stellarator magnetic fields. The possibility of separatrix reconnection occurring is due to the corresponding Hamiltonian being degenerate, which, in our case, corresponds to $\iota' = 0$ in Fig. 11. We note that the homoclinic-type structure shown in Fig. 11 is approached from "above" rather than as a coalescence between two island chains having a heteroclinic-type structure.

Finally, in Fig. 12 and 13 with still higher β, $\beta_0 = 6.5\%$, the value of ι at around half the minor radius decreases down to below 6/5. Accordingly, the homoclinic islands observed in Fig.10 are changed to a pair of heteroclinic (resonant-type) 6/5 island chains. It is interesting to note that the phases of those two island chains are opposite to each other.

IV. CONCLUSION

Using the HINT computer code, we have simulated the evolution of magnetic islands in the H-1 Heliac up to $\beta_0 \approx 6.5\%$. These are the highest plasma pressures to be obtained by an islands code for the difficult Heliac geometry. Our results for a particular H-1 configuration predict an equilibrium limit of $<\beta>$ slightly above 1%. The predicted initial growth, rather than self-healing, of the $\iota = 6/5$ island shown here might be pessimistic for H-1 if the inferred rigidity of the phase of the vacuum islands, and a wider generalization of the earlier results of HINT for other configurations, is confirmed. (We note that a generalization of analytical theory of magnetic island formation to include vacuum islands has verified the phase dependence of self-healing[13].) On the other hand, the observed change of the rotational transform profile with plasma pressure to exclude the resonant surface in question is an optimistic result which might also be generalized to other Heliac configurations. In conclusion, the results in this paper indicate that we should be careful not only on the ordinary resonant-type islands, but also on the near-resonant-type deformation when evaluating equilibrium β limit. The differences in island evolution in the H-1 and TJ-II could form an important part of the experimental program of the two devices.

We note that the homoclinic-type island structure of Fig. 10 has been obtained for the first time in this paper in equilibrium calculations of torus plasmas. Although probably above the equilibrium limit in this particular H-1 case, it might also form an object of study in other low-shear stellarator configurations.

ACKNOWLEDGEMENTS

Part of this research was carried out whilst H.J. Gardner was a visitor at the National Institute for Fusion Science and he wishes to thank the staff of NIFS for their hospitality. The authors are grateful to J.D. Hanson for bringing Ref. 10 to their notice and to R.L. Dewar and J.Nührenberg for valuable discussions.

APPENDIX: SADDLE-NODE BIFURCATION IN A TWIST REVERSING MAP

The flux surfaces have reconnected to form a double island structure that is analogous to the homoclinic phase portraits observed for Hamiltonian systems which have a degeneracy in the mass [12], i.e. where $\partial^2 H/\partial p^2 = 0$; in the present context this is equivalent to a flux surface for which $\iota' = 0$ as occurs in Fig. 11.

A simple model of this phenomena can be obtained using an area preserving map, T, to represent the Poincaré map of the field lines

$$T: \begin{array}{l} y' = y - \frac{k}{2\pi}\sin(2\pi x) \\ x' = x - y'^2 - t \end{array}$$

Here y represents the radial coordinate, and x the poloidal angle (the map is periodic in x with period 1). A map similar to this one has been studied earlier [12,14,15], and can be called the *standard nontwist* map, because the "twist" of this map, $\partial x'/\partial y = 2y$ reverses at $y = 0$. Here we use a slightly different parameterization than the previous papers with a rotational transform $\iota(y) = y^2 - t$. Note that there is no $\iota = 0$ rational surface when $t < 0$. Thus the main driven island in the system, $m/n = 0/1$, does not exist when $t < 0$. Indeed the fixed points of the map, $T(x, y) = (x, y)$ are

$$(0, \sqrt{t}), (0.5, \sqrt{t}), \ \textit{and} \ (0.5, -\sqrt{t}), (0.0, -\sqrt{t})$$

and exist only for positive t. When $k > 0$ the first and third of these points are elliptic (o-points), and the second and forth are hyperbolic(x-points).

The map has the symmetry $S : (x, y) \to (x+1/2, -y)$, i.e. $ST = TS$, so the negative y phase portrait is simply related to that for positive y. The map is also time reversible, $T^{-1} = RTR$ with the involution $R : (x, y) \to (-x, y - \frac{k}{2\pi}\sin(2\pi x))$. This implies that symmetric orbit finding techniques can be used[16].

We show below several phase space plots illustrating the saddle-node bifurcation that occurs when t increases across zero leading to the creation of the two pairs of fixed points. We claim that this is exactly what occurs as β increases from 2% to 6.5% in the simulations. In the first case, when $t < 0$ the flux surfaces show deformations, Fig. 14, that are similar to the field lines in Fig. 8-9.

As t increases past zero, the two pairs of elliptic-hyperbolic fixed points are created, Fig. 15. For small positive t the separatrix of each of the islands has a homoclinic form (unlike the more typical heteroclinic form for nondegenerate systems) : one branch of the unstable manifold of each of the hyperbolic fixed points is homoclinic to the same fixed point, while the other is heteroclinic to the translate ($x \to x+1$) of the fixed point. When $k = 0.3$, this structure occurs for $0 < t < 0.05065$. A similar structure was shown in Fig. 10.

There is a homoclinic bifurcation at $t \approx 0.05065$ where the stable-unstable manifolds of the two x-points appear to join, Fig. 16a (in fact they do not join, as we discuss below). For larger t, the pair of 0/1 islands are far enough from the degeneracy at $y = 0$ that they assume the more standard heteroclinic form, Fig. 16b.

Though the mapping model looks integrable for $k = 0.3$, there are undoubtedly chaotic layers in the neighborhood of the separatrices for any nonzero k. These only become visible at lager values of k, Fig. 17. The chaos is a result of the homoclinic tangles in the stable and unstable manifolds (separatrices) : the stable and unstable manifolds of the two x-points do not smoothly join, rather they cross transversely, leading to the usual sort of heteroclinic tangle. In Fig. 18, we show some of the heteroclinic tangle for $k = 0.8$, just before the homoclinic bifurcation for this value of k which occurs at $t \approx 0.0974$.

REFERENCES

1. K. Harafuji, T. Hayashi, and T. Sato, J. Comput. Phys. **81** 169 (1989).
2. T. Hayashi, T. Sato, and A. Takei, Phys. Fluids B **2** 329 (1990).
3. T. Hayashi, A. Takei, and T. Sato, Phys. Fluids B **4** 1539 (1992).
4. T. Hayashi, T. Sato, W. Lotz, P. Merkel, J. Nührenberg, U. Schwenn, and E. Strumberger, *Proceedings of the 14th International Conference on Plasma Physics and Controlled Nuclear Fusion Research 1992*, Würzburg (International Atomic Energy Agency, Vienna, 1993) Vol. II, p.29.
5. T. Hayashi, T. Sato, P. Merkel, J. Nührenberg, U. Schwenn, to be published in Physics of Plasmas.
6. T. Hayashi, in *Theory of Fusion Plasmas*, Eds. E. Sindoni and J. Vaclavik, EUR 12149 EN 231 (1992).
7. S.M. Hamberger, B.D. Blackwell, L.E. Sharp, and D.B. Shenton, Fusion. Technol. **17** 123 (1990).
8. H.J. Gardner and B.D. Blackwell, Nucl. Fusion **32** 2009 (1992).
9. W.A. Cooper and H.J. Gardner, to appear in Nucl. Fusion.
10. B.D. Blackwell (private communication, 1994).
11. A. Salas, A. López Fraguas, A.H. Reiman, D.A. Monticello, and J.L. Johnson, in *Stellarators and Other Helical Confinement Systems* (Proc. IAEA Tech. Comm. Meeting, Garching, 10-14 May, 1993), IAEA, Vienna p. 127-131 (1993).
12. Diego del-Castillo-Negrete and P.J. Morrison, Phys. Fluids A **5** 948 (1993).
13. A. Bhattacharjee, T. Hayashi, C.C. Hegna, N. Nakajima and T. Sato in preparation for submission to Phys. Plasmas.
14. J. E. Howard and S. M. Mohs, Phys. Rev. **29A** 418 (1984).
15. J. B. Weiss, Phys. Fluids **3A** 1397 (1991).
16. J. M. Greene, J. Math. Phys. **20** 1183 (1997).

FIGURE CAPTIONS

FIG. 1: Poincare plot of the vacuum magnetic field of the H-1 configuration under consideration, at $\phi = 0$ (right) and $\phi = \frac{\pi}{3}$ (left). The solid boundary shows the outer wall on which ideally conducting boundary conditions are imposed for the finite β HINT simulations.

FIG. 2: Rotational transform profile (against average radius from the magnetic axis) for the vacuum configuration of Fig. 1.

FIG. 3: Calculated flux surfaces for $\beta_0 = 1.5\%$.

FIG. 4: Rotational transform profile corresponding to Fig. 3.

FIG. 5: Constant pressure surfaces for the equilibrium of Fig. 3.

FIG. 6: Calculated flux surfaces for $\beta_0 = 2.0\%$.

FIG. 7: Rotational transform profile corresponding to Fig. 6.

FIG. 8: Calculated flux surfaces for $\beta_0 = 3.8\%$.

FIG. 9: Rotational transform profile corresponding to Fig. 8.

FIG. 10: Calculated flux surfaces for $\beta_0 = 4.4\%$.

FIG. 11: Rotational transform profile corresponding to Fig. 10.

FIG. 12: Calculated flux surfaces for $\beta_0 = 6.5\%$.

FIG. 13: Rotational transform profile corresponding to Fig. 12.

FIG. 14: Phase space of the nontwist map for $k = 0.3$. (a) $t = -0.02$ and (b) $t = 0.0$. Coordinates range over $(-.5, .5) \times (-.5, .5)$.

FIG. 15: $k = 0.3$, $t = 0.02$. There are two pairs of elliptic and hyperbolic fixed points at $y = \pm\sqrt{0.02}$.

FIG. 16: $k = 0.3$, (a) $t = 0.05065$ and (b) $t = 0.07$. In (a) there is nearly a homoclinic connection between the positive and negative hyperbolic points. For larger t, the two manifolds are heteroclinic.

FIG. 17: $t = 0.02$, (a) $k = 0.6$ and (b) $k = 0.8$. In (b) the y scale is changed to (-.75,.75). A chaotic layer is visible around the negative y x-point. By symmetry the positive x-point would have an identical layer, but we show the stable and unstable manifolds instead.

FIG. 18: $k = 0.8$, $t = 0.0973$. The heteroclinic tangle in the stable-unstable manifolds.

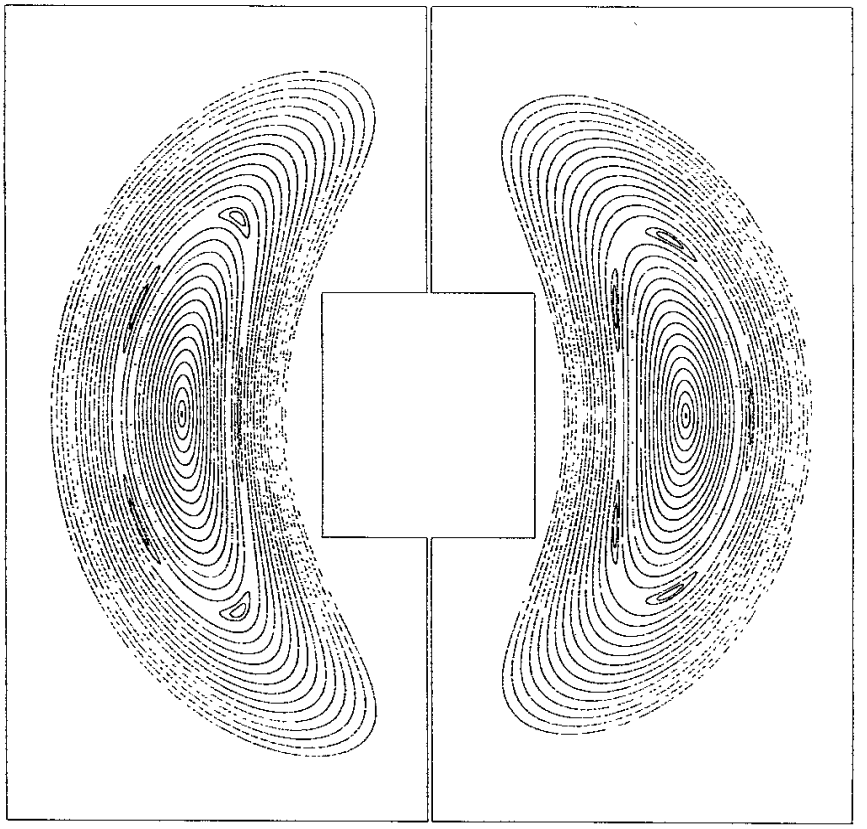

Fig.1

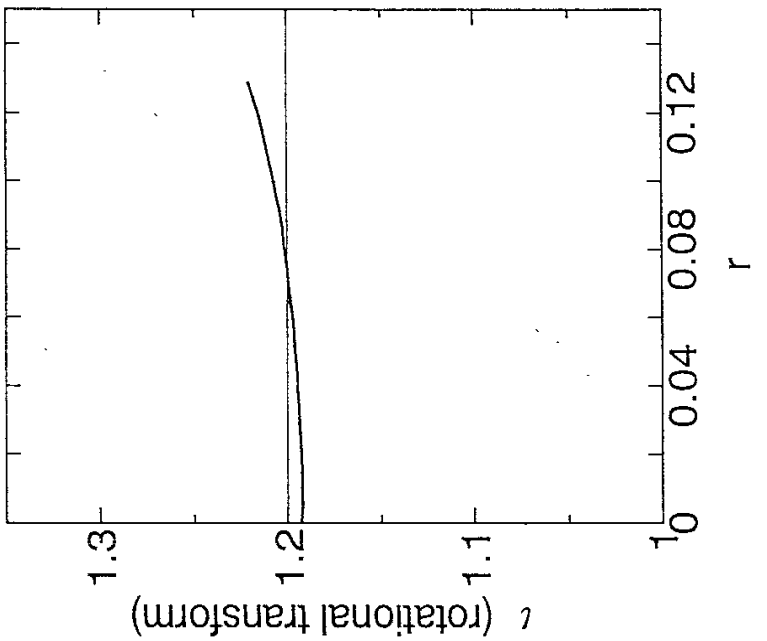

Fig.2

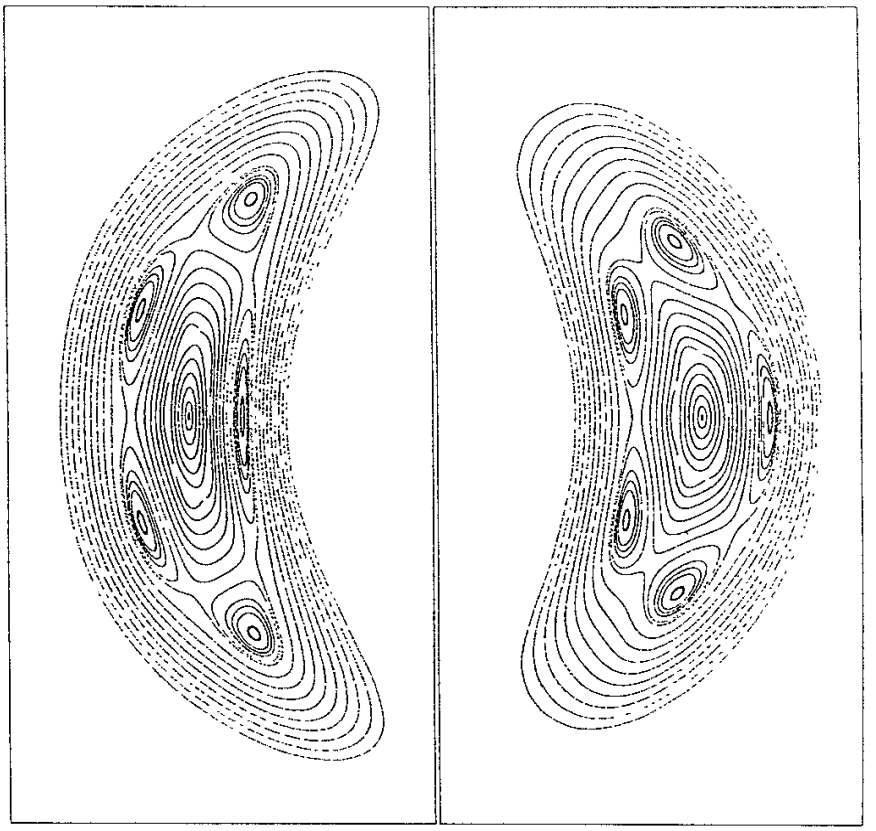

Fig.3

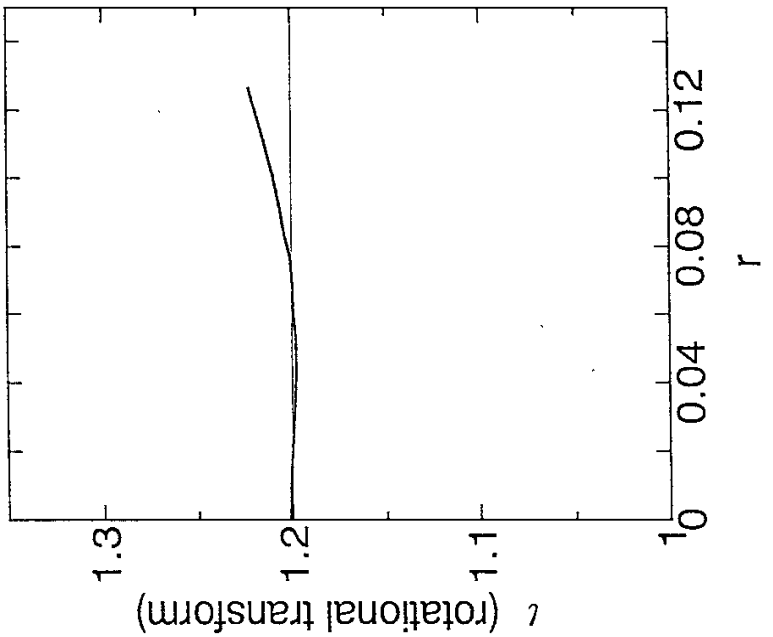

Fig.4

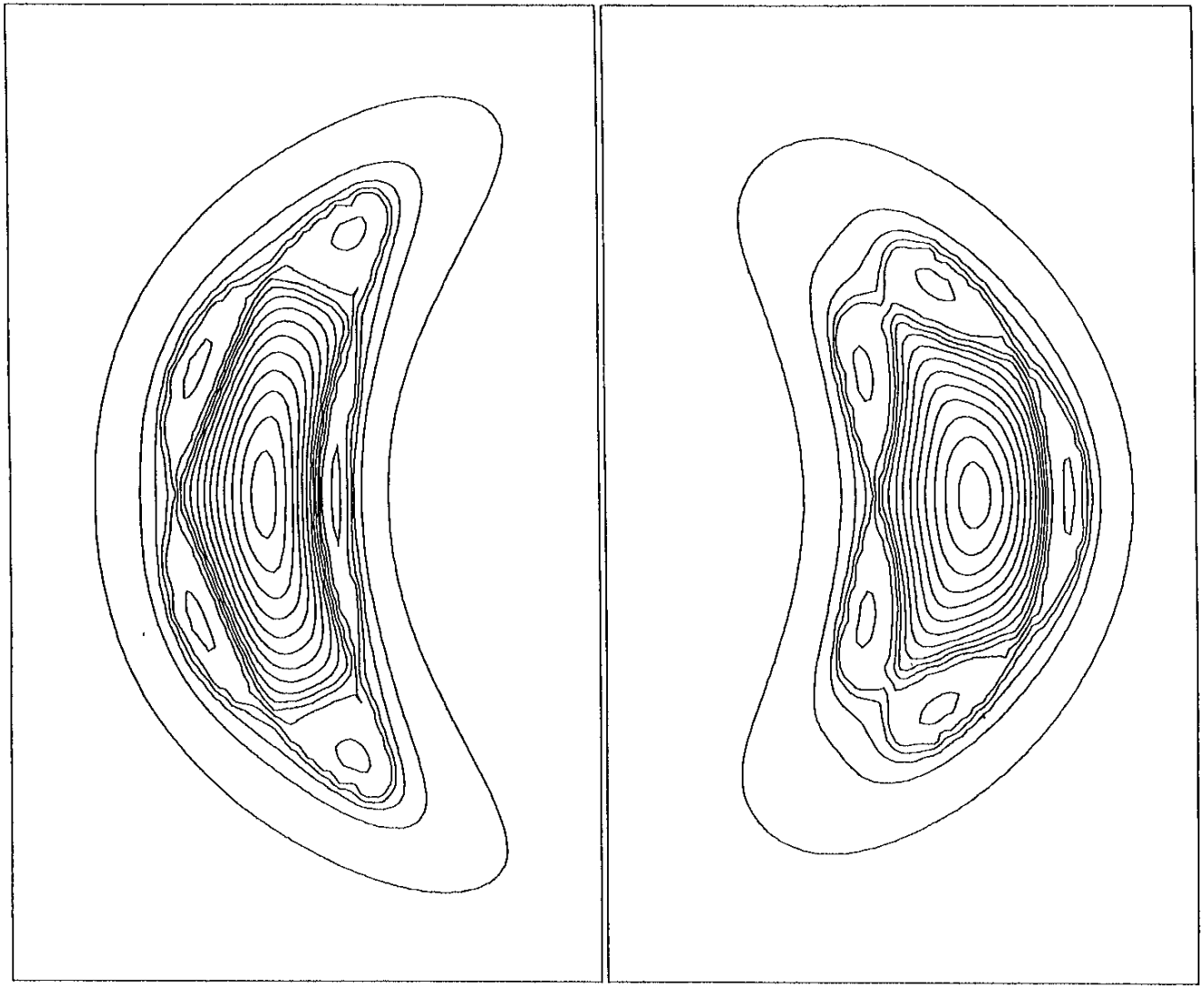

Fig.5

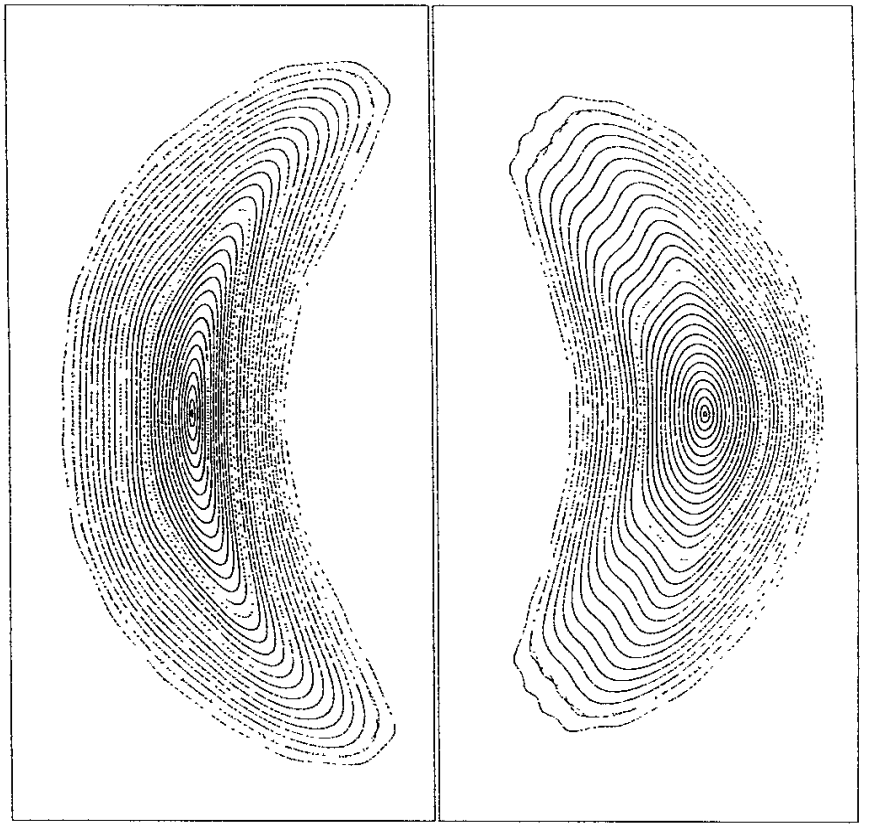

Fig.6

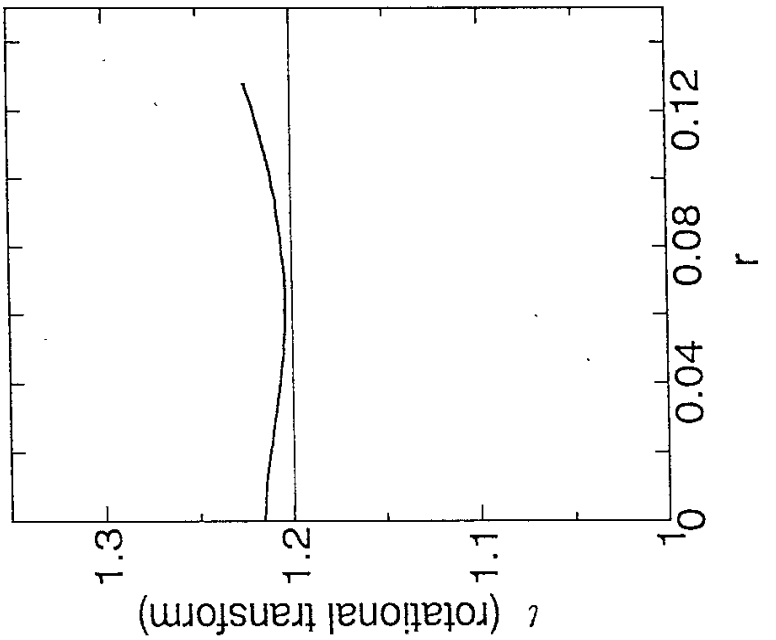

Fig.7

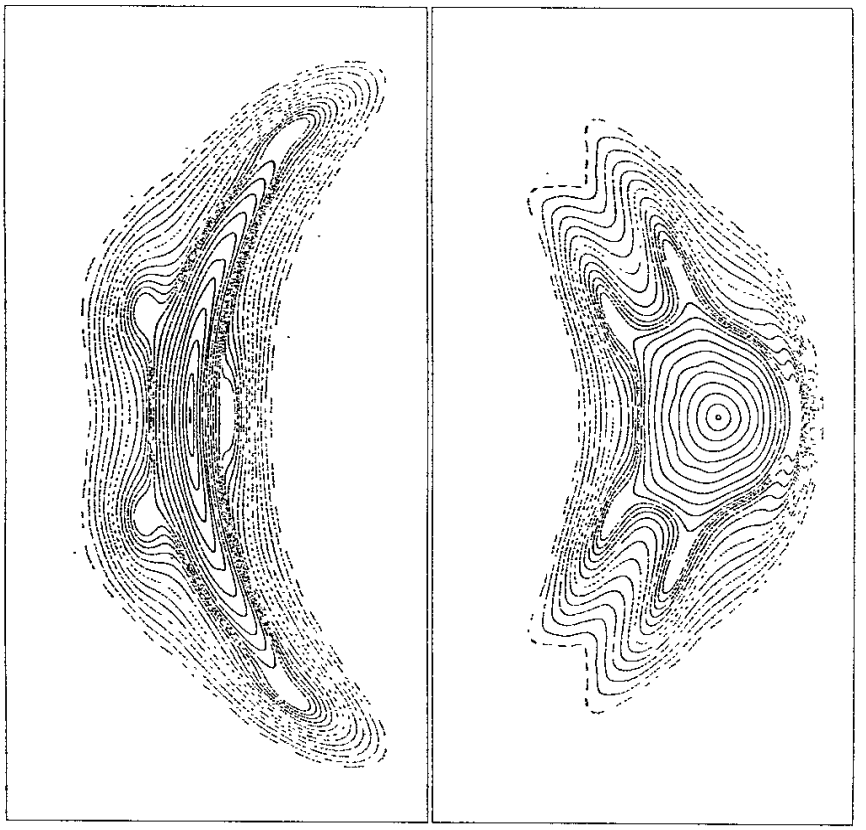

Fig.8

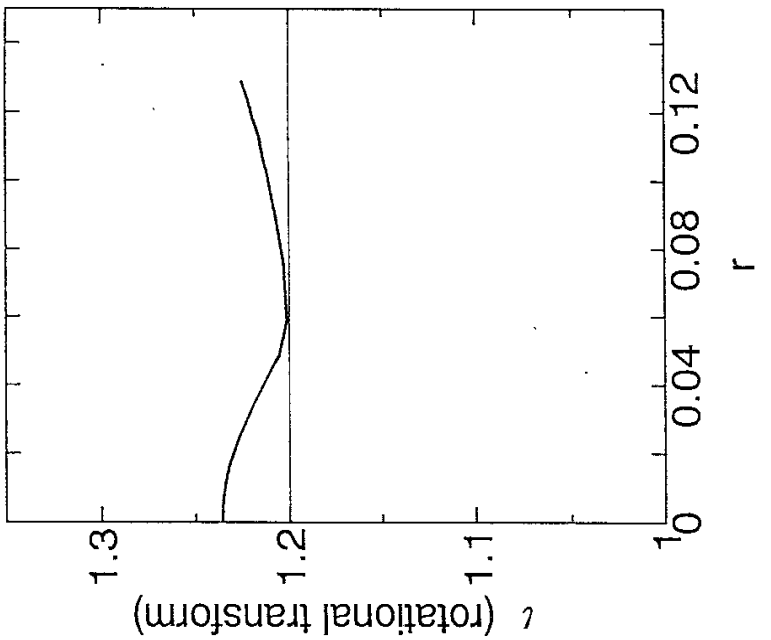

Fig.9

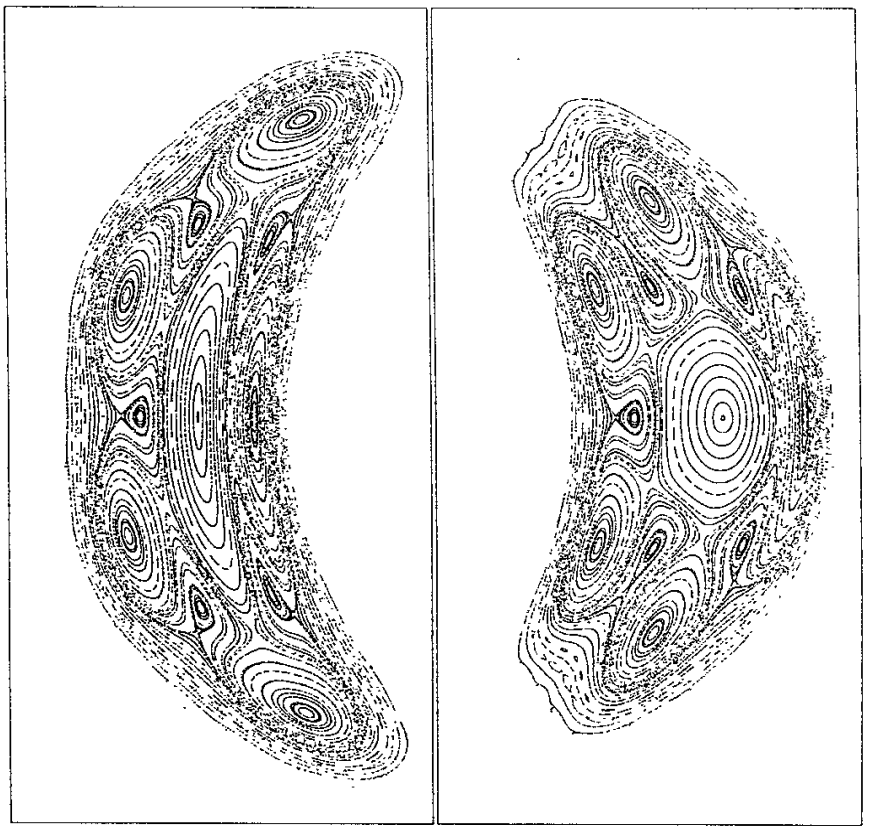

Fig.10

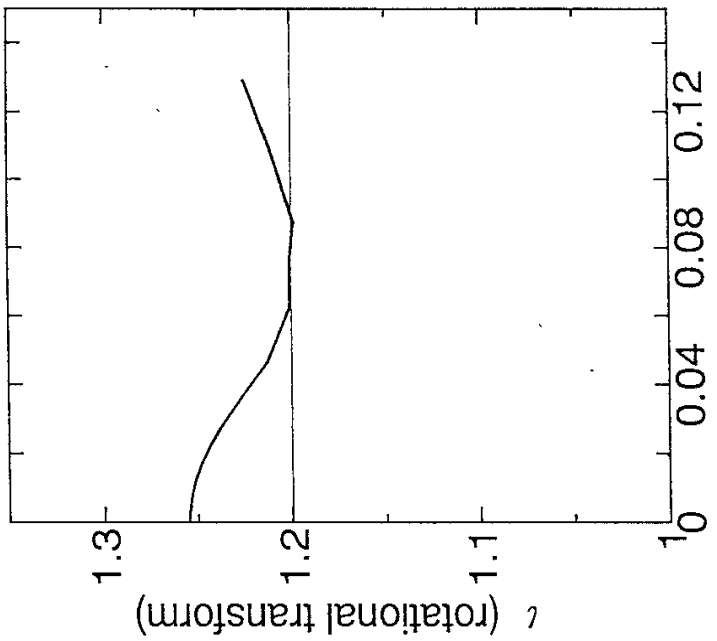

Fig.11

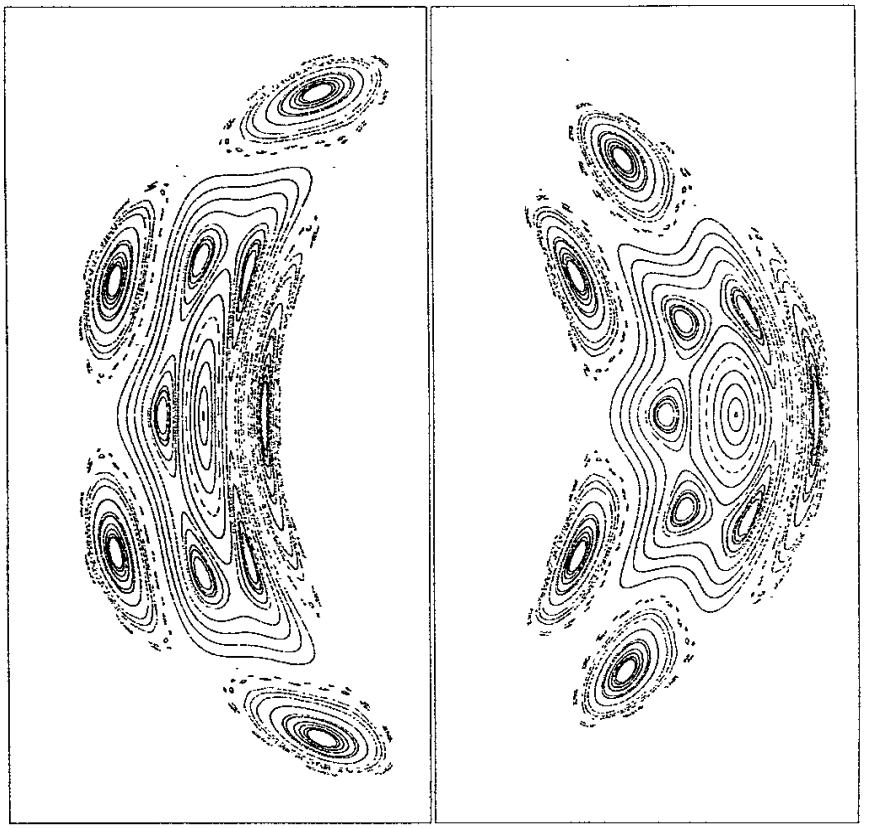

Fig.12

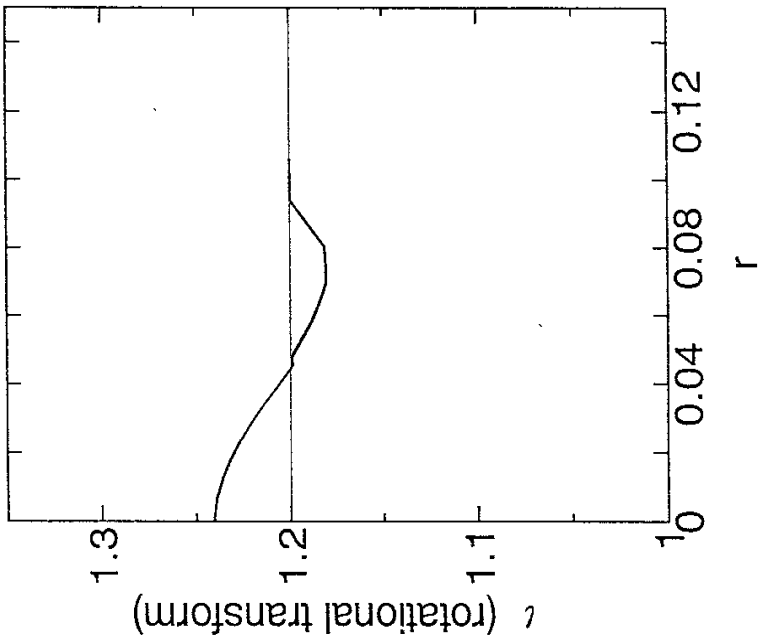

Fig.13

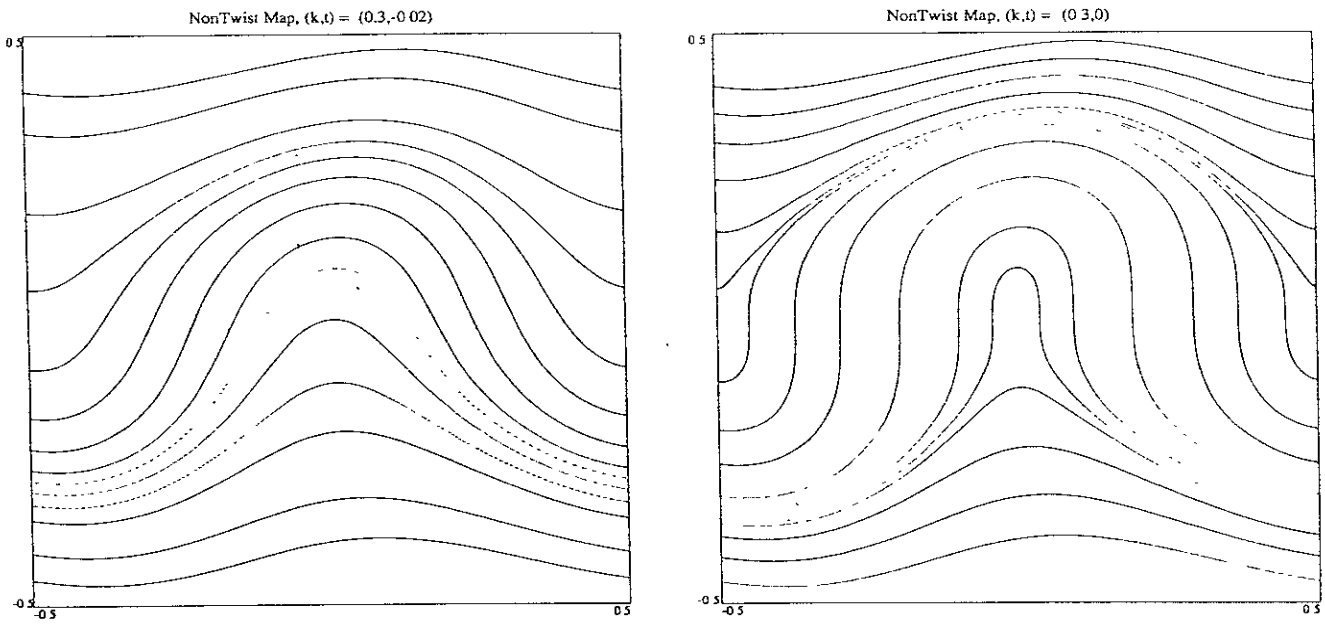
NonTwist Map, (k,t) = (0.3,-0.02)
NonTwist Map, (k,t) = (0.3,0)
0.5
-0.5
0.5
-0.5
0.5
-0.5
0.5
-0.5

Fig.14

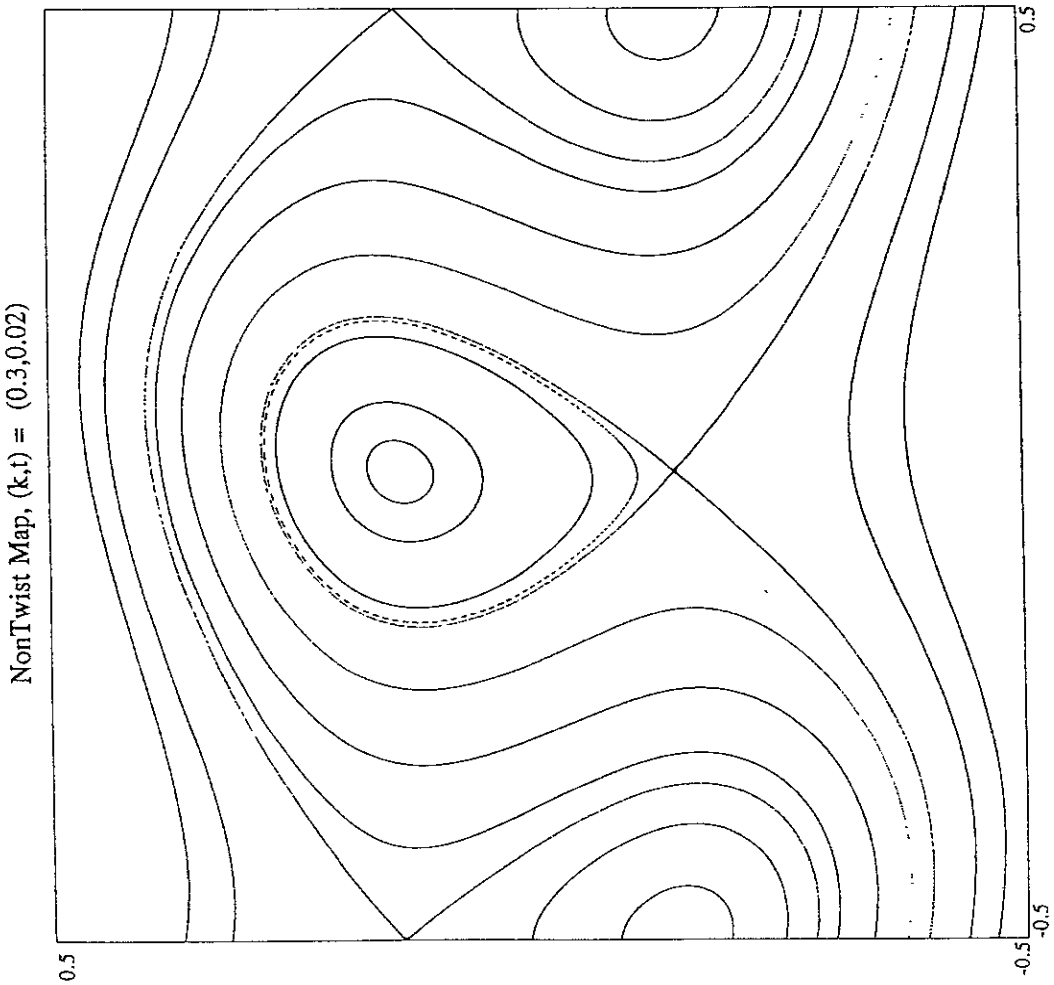
NonTwist Map, (k,t) = (0.3,0.02)
0.5
0.5
-0.5
-0.5

Fig.15

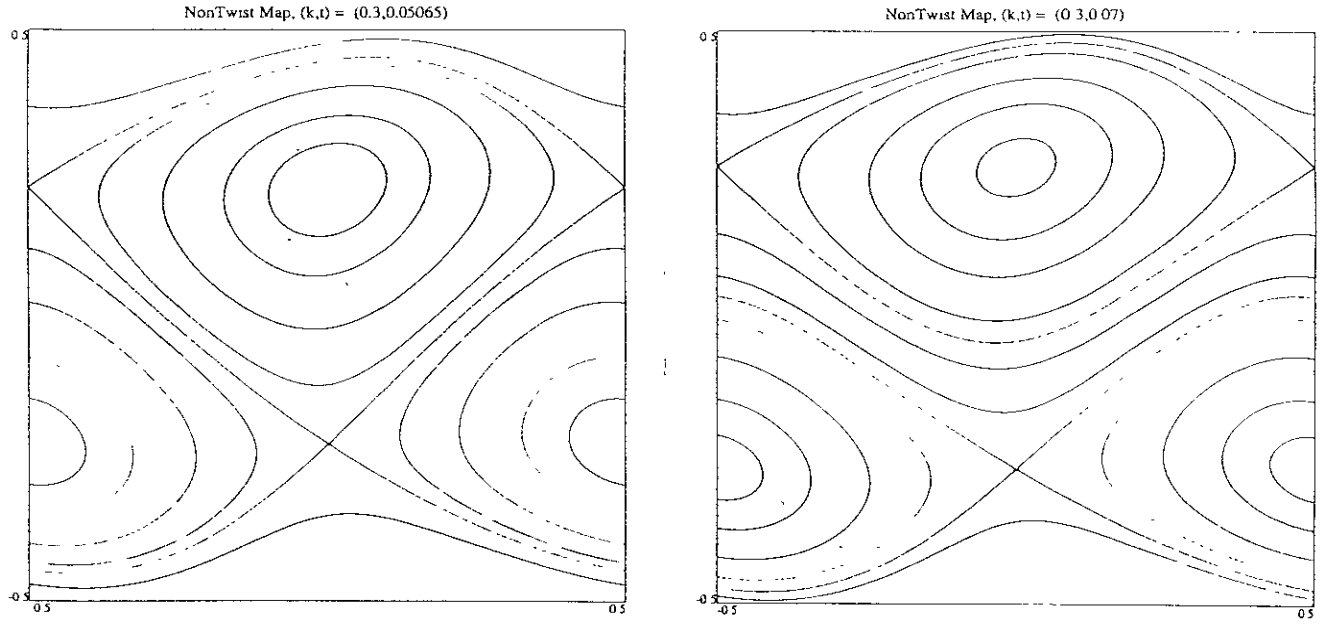
NonTwist Map, (k,t) = (0.3,0.05065)
NonTwist Map, (k,t) = (0 3,0 07)

Fig.16

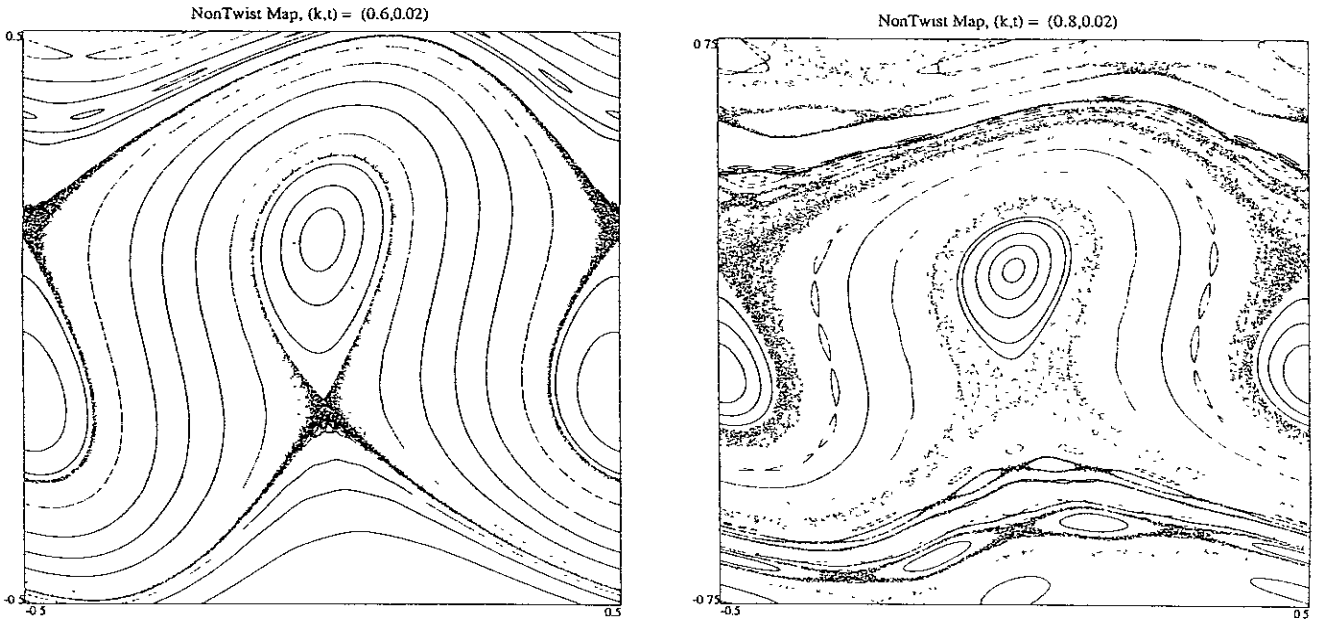
NonTwist Map, (k,t) = (0.6,0.02)
NonTwist Map, (k,t) = (0.8,0.02)

Fig.17

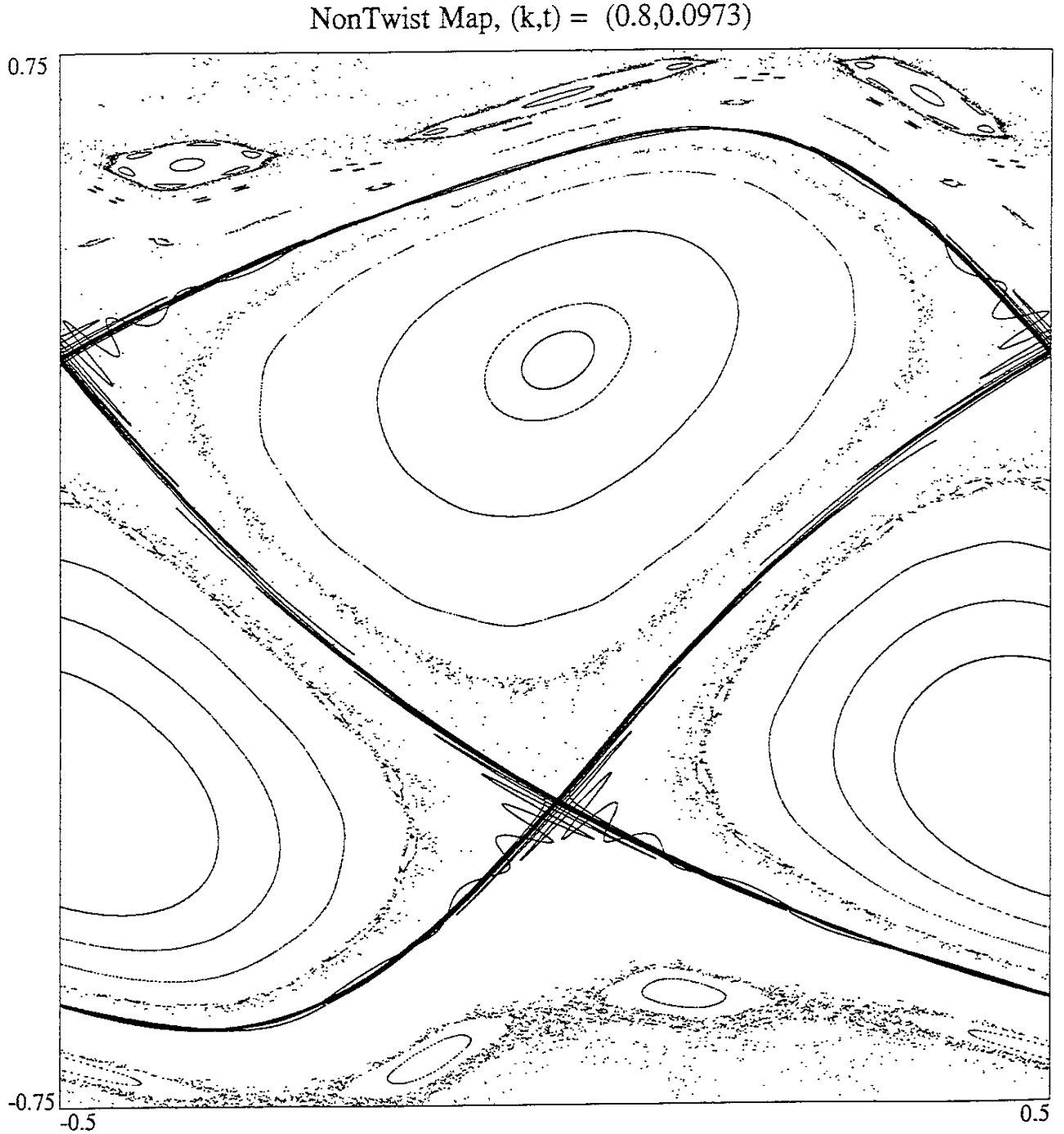

Fig.18

Recent Issues of NIFS Series

NIFS-271 Y. Nejoh, H. Sanuki,
Large Amplitude Langmuir and Ion-Acoustic Waves in a Relativistic Two-Fluid Plasma; Feb. 1994

NIFS-272 A. Fujisawa, H. Iguchi, A. Taniike, M. Sasao, Y. Hamada,
A 6MeV Heavy Ion Beam Probe for the Large Helical Device;
Feb. 1994

NIFS-273 Y. Hamada, A. Nishizawa, Y. Kawasumi, K. Narihara, K. Sato, T. Seki, K. Toi, H. Iguchi, A. Fujisawa, K. Adachi, A. Ejiri, S. Hidekuma, S. Hirokura, K. Ida, J. Koong, K. Kawahata, M. Kojima, R. Kumazawa, H. Kuramoto, R. Liang, H. Sakakita, M. Sasao, K. N. Sato, T. Tsuzuki, J. Xu, I. Yamada, T. Watari, I. Negi,
Measurement of Profiles of the Space Potential in JIPP T-IIU Tokamak Plasmas by Slow Poloidal and Fast Toroidal Sweeps of a Heavy Ion Beam; Feb. 1994

NIFS-274 M. Tanaka,
A Mechanism of Collisionless Magnetic Reconnection; Mar. 1994

NIFS-275 A. Fukuyama, K. Itoh, S.-I. Itoh, M. Yagi and M. Azumi,
Isotope Effect on Confinement in DT Plasmas; Mar. 1994

NIFS-276 R.V. Reddy, K. Watanabe, T. Sato and T.H. Watanabe,
Impulsive Alfven Coupling between the Magnetosphere and Ionosphere;
Apr.1994

NIFS-277 J. Uramoto,
A Possibility of π^- Meson Production by a Low Energy Electron Bunch and Positive Ion Bunch; Apr. 1994

NIFS-278 K. Itoh, S.-I. Itoh, A. Fukuyama, M. Yagi and M. Azumi,
Self-sustained Turbulence and L-mode Confinement in Toroidal Plasmas II; Apr. 1994

NIFS-279 K. Yamazaki and K.Y.Watanabe,
New Modular Heliotron System Compatible with Closed Helical Divertor and Good Plasma Confinement; Apr. 1994

NIFS-280 S. Okamura, K. Matsuoka, K. Nishimura, K. Tsumori, R. Akiyama, S. Sakakibara, H. Yamada, S. Morita, T. Morisaki,. N. Nakajima, K. Tanaka, J. Xu, K. Ida, H. Iguchi, A. Lazaros, T. Ozaki, H. Arimoto, A. Ejiri, M. Fujiwara, H. Idei. O. Kaneko, K. Kawahata, T. Kawamoto, A. Komori, S. Kubo, O. Motojima, V.D. Pustovitov, C. Takahashi, K. Toi and I. Yamada,
High-Beta Discharges with Neutral Beam Injection in CHS; Apr. 1994

NIFS-281 K. Kamada, H. Kinoshita and H. Takahashi,
Anomalous Heat Evolution of Deuteron Implanted Al on Electron Bombardment ; May 1994

NIFS-282 H. Takamaru, T. Sato, K. Watanabe and R. Horiuchi,
Super Ion Acoustic Double Layer; May 1994

NIFS-283 O.Mitarai and S. Sudo
Ignition Characteristics in D-T Helical Reactors; June 1994

NIFS-284 R. Horiuchi and T. Sato,
Particle Simulation Study of Driven Magnetic Reconnection in a Collisionless Plasma; June 1994

NIFS-285 K.Y. Watanabe, N. Nakajima, M. Okamoto, K. Yamazaki, Y. Nakamura, M. Wakatani,
Effect of Collisionality and Radial Electric Field on Bootstrap Current in LHD (Large Helical Device); June 1994

NIFS-286 H. Sanuki, K. Itoh, J. Todoroki, K. Ida, H. Idei, H. Iguchi and H. Yamada,
Theoretical and Experimental Studies on Electric Field and Confinement in Helical Systems; June 1994

NIFS-287 K. Itoh and S-I. Itoh,
Influence of the Wall Material on the H-mode Performance; June 1994

NIFS-288 K. Itoh, A. Fukuyama, S.-I. Itoh, M. Yagi and M. Azumi
Self-Sustained Magnetic Braiding in Toroidal Plasmas: July 1994

NIFS-289 Y. Nejoh,
Relativistic Effects on Large Amplitude Nonlinear Langmuir Waves in a Two-Fluid Plasma; July 1994

NIFS-290 N. Ohyabu, A. Komori, K. Akaishi, N. Inoue, Y. Kubota, A.I. Livshit, N. Noda, A. Sagara, H. Suzuki, T. Watanabe, O. Motojima, M. Fujiwara, A. Iiyoshi,
Innovative Divertor Concepts for LHD; July 1994

NIFS-291 H. Idei, K. Ida, H. Sanuki, S. Kubo, H. Yamada, H. Iguchi, S. Morita, S. Okamura, R. Akiyama, H. Arimoto, K. Matsuoka, K. Nishimura, K. Ohkubo, C. Takahashi, Y. Takita, K. Toi, K. Tsumori and I. Yamada,
Formation of Positive Radial Electric Field by Electron Cyclotron Heating in Compact Helical System; July 1994

NIFS-292 N. Noda, A. Sagara, H. Yamada, Y. Kubota, N. Inoue, K. Akaishi, O. Motojima, K. Iwamoto, M. Hashiba, I. Fujita, T. Hino, T. Yamashina, K. Okazaki, J. Rice, M. Yamage, H. Toyoda and H. Sugai,

Boronization Study for Application to Large Helical Device; July 1994

NIFS-293 Y. Ueda, T. Tanabe, V. Philipps, L. Könen, A. Pospieszczyk, U. Samm, B. Schweer, B. Unterberg, M. Wada, N. Hawkes and N. Noda, *Effects of Impurities Released from High Z Test Limiter on Plasma Performance in TEXTOR*; July. 1994

NIFS-294 K. Akaishi, Y. Kubota, K. Ezaki and O. Motojima, *Experimental Study on Scaling Law of Outgassing Rate with A Pumping Parameter*, Aug. 1994

NIFS-295 S. Bazdenkov, T. Sato, R. Horiuchi, K. Watanabe *Magnetic Mirror Effect as a Trigger of Collisionless Magnetic Reconnection*, Aug. 1994

NIFS-296 K. Itoh, M. Yagi, S.-I. Itoh, A. Fukuyama, H. Sanuki, M. Azumi *Anomalous Transport Theory for Toroidal Helical Plasmas*, Aug. 1994 (IAEA-CN-60/D-III-3)

NIFS-297 J. Yamamoto, O. Motojima, T. Mito, K. Takahata, N. Yanagi, S. Yamada, H. Chikaraishi, S. Imagawa, A. Iwamoto, H. Kaneko, A. Nishimura, S. Satoh, T. Satow, H. Tamura, S. Yamaguchi, K. Yamazaki, M. Fujiwara, A. Iiyoshi and LHD group, *New Evaluation Method of Superconductor Characteristics for Realizing the Large Helical Device;* Aug. 1994 (IAEA-CN-60/F-P-3)

NIFS-298 A. Komori, N. Ohyabu, T. Watanabe, H. Suzuki, A. Sagara, N. Noda, K. Akaishi, N. Inoue, Y. Kubota, O Motojima, M. Fujiwara and A. Iiyoshi, *Local Island Divertor Concept for LHD*; Aug. 1994 (IAEA-CN-60/F-P-4)

NIFS-299 K. Toi, T. Morisaki, S. Sakakibara, A. Ejiri, H. Yamada, S. Morita, K. Tanaka, N. Nakjima, S. Okamura, H. Iguchi, K. Ida, K. Tsumori, S. Ohdachi, K. Nishimura, K. Matsuoka, J. Xu, I. Yamada, T. Minami, K. Narihara, R. Akiyama, A. Ando, H. Arimoto, A. Fujisawa, M. Fujiwara, H. Idei, O. Kaneko, K. Kawahata, A. Komori, S. Kubo, R. Kumazawa, T. Ozaki, A. Sagara, C. Takahashi, Y. Takita and T. Watari *Impact of Rotational-Transform Profile Control on Plasma Confinement and Stability in CHS*; Aug. 1994 (IAEA-CN-60/A6/C-P-3)

NIFS-300 H. Sugama and W. Horton, *Dynamical Model of Pressure-Gradient-Driven Turbulence and Shear Flow Generation in L-H Transition;* Aug. 1994 (IAEA/CN-60/D-P-I-11)

NIFS-301 Y. Hamada, A. Nishizawa, Y. Kawasumi, K.N. Sato, H. Sakakita, R. Liang, K. Kawahata, A. Ejiri, K. Narihara, K. Sato, T. Seki, K. Toi, K. Itoh, H. Iguchi, A. Fujisawa, K. Adachi, S. Hidekuma, S. Hirokura, K. Ida, M. Kojima, J. Koog, R. Kumazawa, H. Kuramoto, T. Minami, I. Negi, S. Ohdachi, M. Sasao, T. Tsuzuki, J. Xu, I. Yamada, T. Watari, *Study of Turbulence and Plasma Potential in JIPP T-IIU Tokamak*;

Aug. 1994 (IAEA/CN-60/A-2-III-5)

NIFS-302 K. Nishimura, R. Kumazawa, T. Mutoh, T. Watari, T. Seki, A. Ando, S. Masuda, F. Shinpo, S. Murakami, S. Okamura, H. Yamada, K. Matsuoka, S. Morita, T. Ozaki, K. Ida, H. Iguchi, I. Yamada, A. Ejiri, H. Idei, S. Muto, K. Tanaka, J. Xu, R. Akiyama, H. Arimoto, M. Isobe, M. Iwase, O. Kaneko, S. Kubo, T. Kawamoto, A. Lazaros, T. Morisaki, S. Sakakibara, Y. Takita, C. Takahashi and K. Tsumori,
ICRF Heating in CHS; Sep. 1994 (IAEA-CN-60/A-6-I-4)

NIFS-303 S. Okamura, K. Matsuoka, K. Nishimura, K. Tsumori, R. Akiyama, S. Sakakibara, H. Yamada, S. Morita, T. Morisaki, N. Nakajima, K. Tanaka, J. Xu, K. Ida, H. Iguchi, A. Lazaros, T. Ozaki, H. Arimoto, A. Ejiri, M. Fujiwara, H. Idei, A. Iiyoshi, O, Kaneko, K. Kawahata, T. Kawamoto, S. Kubo, T. Kuroda, O. Motojima, V.D. Pustovitov, A. Sagara, C. Takahashi, K. Toi and I. Yamada,
High Beta Experiments in CHS; Sep. 1994 (IAEA-CN-60/A-2-IV-3)

NIFS-304 K. Ida, H. Idei, H. Sanuki, K. Itoh, J. Xu, S. Hidekuma, K. Kondo, A. Sahara, H. Zushi, S.-I. Itoh, A. Fukuyama, K. Adati, R. Akiyama, S. Bessho, A. Ejiri, A. Fujisawa, M. Fujiwara, Y. Hamada, S. Hirokura, H. Iguchi, O. Kaneko, K. Kawahata, Y. Kawasumi, M. Kojima, S. Kubo, H. Kuramoto, A. Lazaros, R. Liang, K. Matsuoka, T. Minami, T. Mizuuchi, T. Morisaki, S. Morita, K. Nagasaki, K. Narihara, K. Nishimura, A. Nishizawa, T. Obiki, H. Okada, S. Okamura, T. Ozaki, S. Sakakibara, H. Sakakita, A. Sagara, F. Sano, M. Sasao, K. Sato, K.N. Sato, T. Saeki, S. Sudo, C. Takahashi, K. Takaka, K. Tsumori, H.Yamada, I. Yamada, Y. Takita, T. Tuzuki, K. Toi and T. Watari,
Control of Radial Electric Field in Torus Plasma; Sep. 1994
(IAEA-CN-60/A-2-IV-2)

NIFS-305 T. Hayashi, T. Sato, N. Nakajima, K. Ichiguchi, P. Merkel, J. Nührenberg, U. Schwenn, H. Gardner, A. Bhattacharjee and C.C.Hegna,
Behavior of Magnetic Islands in 3D MHD Equilibria of Helical Devices;
Sep. 1994 (IAEA-CN-60/D-2-II-4)

NIFS-306 S. Murakami, M. Okamoto, N. Nakajima, K.Y. Watanabe, T. Watari, T. Mutoh, R. Kumazawa and T. Seki,
Monte Carlo Simulation for ICRF Heating in Heliotron/Torsatrons;
Sep. 1994 (IAEA-CN-60/D-P-I-14)

NIFS-307 Y. Takeiri, A. Ando, O. Kaneko, Y. Oka, K. Tsumori, R. Akiyama, E. Asano, T. Kawamoto, T. Kuroda, M. Tanaka and H. Kawakami
Development of an Intense Negative Hydrogen Ion Source with a Wide-Range of External Magnetic Filter Field; Sep. 1994